Research Square

Preprints are preliminary reports that have not undergone peer review.
They should not be considered conclusive, used to inform clinical practice,
or referenced by the media as validated information.

Accumulated-History Replicator SelectionOptimization: Algorithm Design, TheoreticalGrounding, and Experimental Analysis (MycelialNetwork Optimization)

Rahul Kumar Mishra

mishra.rahul98@gmail.com

Independent Researcher Ranchi

Article

Keywords:

Posted Date: July 6th, 2026

DOI: https://doi.org/10.21203/rs.3.rs-10057353/v1

License: This work is licensed under a Creative Commons Attribution 4.0 International License.
Read Full License

Additional Declarations: No competing interests reported.

Version of Record: A version of this preprint was published at Scientific Reports on September 26th, 2026. See the published version at https://doi.org/10.1038/s41598-026-73273-5.

Accumulated-History Replicator Selection Optimization: Algorithm Design, Theoretical Grounding, and Experimental Analysis (Mycelial Network Optimization)

Rahul Kumar Mishra[1,*]

[1]Independent Researcher, Mishra House, Ranchi, Jharkhand, India 834012. ORCID: 0009-0004-9671-4055
[*]mishra.rahul98@gmail.com

ABSTRACT

Population-based optimisation algorithms typically decide which candidate solutions survive using only their fitness at the current iteration, discarding all earlier performance information. This memoryless design forfeits a source of signal that biological selection systems routinely exploit: the persistence of quality over time. Here the Accumulated-History Replicator Selection (AHRS) framework is introduced, together with its algorithmic implementation, Mycelial Network Optimization (MNO), which maintains an exponentially weighted history of each candidate's quality and uses this accumulated value, rather than instantaneous fitness, as the survival criterion. This update rule is shown to be the Euler discretisation of the Replicator Equation from evolutionary game theory, with a quantified truncation error, and to guarantee non-decreasing expected population quality through Fisher's Fundamental Theorem. Across twenty classical benchmark functions, fifteen CEC 2017 functions, and six engineering design problems, MNO outperforms Particle Swarm Optimization and Differential Evolution on structured, non-separable landscapes, while honestly under-performing parameter-adaptive variants such as SHADE, JADE and L-SHADE on smooth separable functions. Ablation experiments confirm that both algorithmic operators contribute independently to performance. These results identify accumulated history as a previously unexploited and theoretically grounded selection signal for population-based optimisation.

1 Introduction

The majority of population-based optimisation algorithms make a critical architectural choice that goes largely unquestioned: whether a candidate solution survives into the next generation is decided purely on the basis of its fitness at time t. Particle Swarm Optimization (PSO)[2] directs particles toward the current personal best and global best; Differential Evolution (DE)[3] replaces a parent vector only if the trial vector is strictly better right now; SHADE[22] and L-SHADE[27] maintain a success history of *parameter* values but still evaluate individual survival on current fitness alone. An agent that has occupied the top decile of the population for fifty consecutive iterations is treated identically to a randomly generated newcomer with a marginally better current fitness value. This temporal blindness is structurally universal across the field.

On smooth, separable landscapes, current fitness is a sufficient statistic for survival decisions. On structured, non-separable landscapes, however, past performance carries information about landscape geometry that current fitness alone does not reveal. Discarding this temporal dimension forfeits a source of signal that biological selection systems routinely exploit.

Swarm and evolutionary computation has expanded substantially in recent years, and the resulting landscape of nature-inspired algorithms has been surveyed extensively[18]. The Harris Hawks Optimizer[6] models cooperative raptor hunting with an energy-based phase transition between exploration and exploitation. The Slime Mould Algorithm[1] captures the oscillatory weight adjustment of *Physarum polycephalum* during network formation through a fitness-ranked wrapping function. The Arithmetic Optimization Algorithm[21] distributes the population across the search space using elementary arithmetic operators, and further additions to this family include the Whale Optimization Algorithm[16], the Honey Badger Algorithm[17], the cuckoo search family[19], the Butterfly Optimization Algorithm[20], the Multi-Verse Optimizer[25], and Wind Driven Optimization[31]. Among Differential Evolution variants, SHADE[22] and its successor L-SHADE[27] represent the current state of the art: SHADE maintains a historical archive of successful parameter values and updates the crossover rate and scaling factor using Lehmer-mean weighting, while L-SHADE adds a linear population-size-reduction strategy that has won multiple CEC competitions[24]. JADE[23] uses adaptive control of the mean crossover rate and scaling factor with separate success archives, and Differential Evolution more broadly has been the subject of extensive theoretical analysis[33]. Hybridised metaheuristics combining several of these mechanisms have in turn been applied across domains ranging from multi-objective engineering optimisation[8] to

renewable-energy parameter identification[9]. None of these algorithms, however different their search operators or application domain, changes the underlying survival rule: selection is decided from the current generation's fitness alone.

A small number of mechanisms touch on temporal accumulation without fully exploiting it. Fitness inheritance[15] maintains smoothed fitness estimates across generations to reduce evaluation cost, using exponential moving averages of past evaluations at spatially nearby points; this is the closest existing mechanism to the streaming update introduced below, but it governs evaluation cost rather than survival probability, and the averaging is over spatial proximity rather than an individual agent's own temporal trajectory. Estimation of Distribution Algorithms[26] learn a probabilistic model of the distribution of good solutions and accumulate statistical information at the population level rather than at the level of individual trajectories. Aging mechanisms[15] remove agents after a fixed number of iterations – a discrete, binary mechanism that is unrelated to accumulated performance – and immune-memory algorithms[34] maintain an archive of previously successful solutions without grading individual long-term productivity. The Replicator Equation[28] of evolutionary game theory describes how strategy frequencies evolve under selection and has been studied extensively in mathematical biology; to our knowledge, no prior metaheuristic algorithm has had its individual-level selection mechanism explicitly formulated as a discretisation of the Replicator Equation with formally verified error bounds.

This paper introduces the **Accumulated-History Replicator Selection (AHRS)** framework, implemented as the **Mycelial Network Optimization (MNO)** algorithm. The biological inspiration – fungal mycelia accumulate cytoplasmic resources over time and share them via anastomosis – provides an intuitive motivation, but the biological framing is secondary to the mathematical formulation. The central theoretical result is that the AHRS streaming update is the Euler discretisation of the Replicator Equation, with formally bounded truncation error and known convergence properties through Fisher's Fundamental Theorem[29], connecting MNO to a well-studied body of mathematical theory rather than to a biological metaphor alone. Four contributions are made: (1) a formally history-dependent selection criterion, together with a proof that it is not memoryless; (2) a formal connection to the Replicator Equation with quantified, $O(\gamma^2)$ error bounds and explicit assumption statements; (3) a structured ablation protocol confirming that both algorithmic operators contribute independently; and (4) a comprehensive experimental evaluation against seven baseline algorithms, including a Nemenyi critical-difference analysis and a parameter sensitivity study. The novelty claim is deliberately bounded: MNO does not claim novelty for exponential smoothing per se, nor for biologically inspired movement rules, nor for the Replicator Equation itself, but for the specific combination of individually accumulated exponential quality history used directly as a survival criterion, with its dynamics formally connected to evolutionary game theory.

2 Results

2.1 Algorithm overview

MNO maintains, for every agent i, a position x_i and a resource variable R_i. Two coupled operators govern the population: *cytoplasmic streaming*, which updates R_i as an exponentially weighted moving average of the agent's quality history and removes agents whose accumulated resource falls below a budget-dependent threshold, and *fitness-proximity anastomosis*, which pairs agents occupying similar fitness niches for resource transfer and a greedy chemotactic repositioning step. Movement additionally uses a resource-weighted natural-gradient step that elongates the search ellipse along high-variance, typically more productive, search directions. Figure 1 summarises the biological motivation, the two operator equations, and the resulting replicator-style convergence of resource weights toward high-quality agents; full equations and the complete pseudocode are given in Methods.

2.2 Theoretical guarantees

Two formal results underpin MNO's design (full derivations and proofs are given in Methods). First, the resource variable $R_i(t)$ is a sufficient statistic for an agent's complete past quality trajectory and cannot be expressed as a function of current quality alone: two agents with identical instantaneous quality but different histories have different resources, and therefore different survival probabilities. This formally establishes that the survival criterion is history-dependent rather than memoryless (Theorem 1).

Second, writing $p_i(t) = R_i(t)/\sum_j R_j(t)$ for the normalised resource weight, the streaming update's continuous-time limit corresponds exactly to the Replicator Equation of evolutionary game theory,

$$\frac{dp_i}{dt} = \gamma p_i \left(Q_i - \bar{Q}\right), \tag{1}$$

with a local truncation error bounded by $O(\gamma^2)$ and Euler-scheme stability for all streaming rates $\gamma \in (0,1)$ (Theorem 2). A direct corollary, via Fisher's Fundamental Theorem, is that the resource-weighted mean quality $\bar{Q}(t)$ is non-decreasing in expectation throughout the run. Equation (1) situates MNO's selection rule within a well-studied body of mathematical theory rather than within a biological metaphor alone, and is the formal basis for the empirical results that follow.

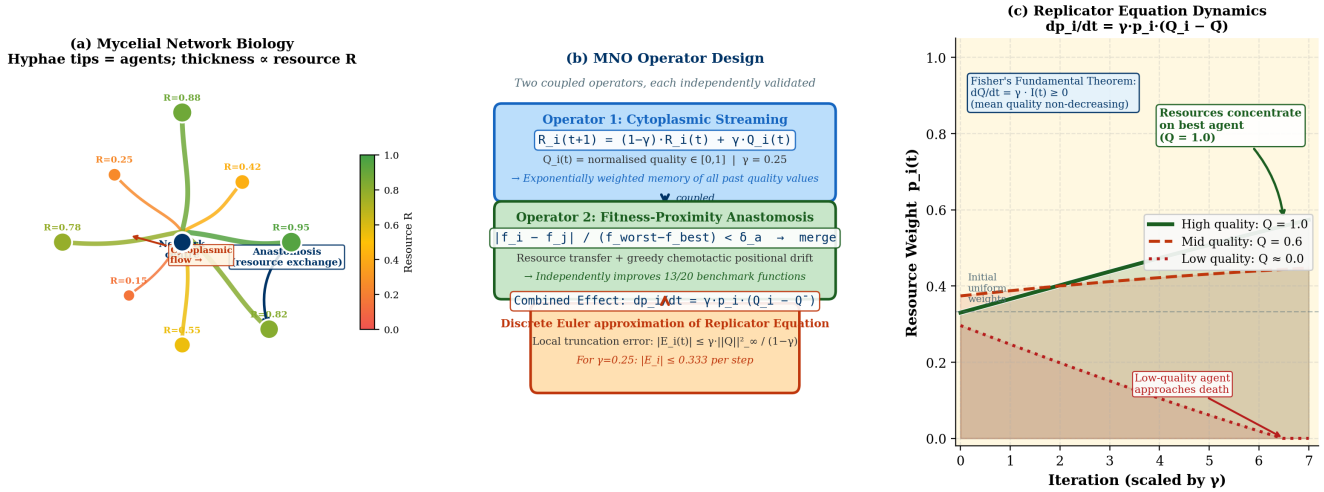


Figure 1. Mycelial Network Optimization: biological inspiration, operator design, and theoretical foundation. (a) Simulated mycelial network with resource-weighted nodes and directed cytoplasmic flow. (b) Formal operator equations. (c) Replicator Equation dynamics: resource weights converge to concentration on high-quality agents.

2.3 Ablation study

Table 1 reports an ablation across four configurations – a movement-only baseline (BASE), BASE with anastomosis only, BASE with streaming only, and the complete MNO algorithm – using identical population size, function-evaluation budget, and random seeds, so that differences are attributable solely to the operators under test.

Streaming independently improves 9/20 functions (mean log-decade gain 0.826). The functions that benefit share a common landscape property: persistent occupation of productive regions over time provides genuine signal about long-term quality. On Trigonometric, sustained streaming pressure concentrates resources in the productive basin far more effectively than any single-iteration decision; on Schwefel 1.2 and 2.22, the strong variable coupling means a good solution at iteration t is likely to remain good at $t+5$ and $t+10$.

Anastomosis independently improves 13/20 functions (mean gain 0.500). Its broader reach reflects that inter-agent resource transfer and chemotactic repositioning benefit any function with fitness-niche structure, even without persistent quality regions. The five functions where neither operator helps (Sphere, Griewank, Camel Back, Branin, Goldstein–Price) are smooth, separable, or very low-dimensional – precisely where theory predicts no benefit, since current fitness is already a sufficient statistic. The combined algorithm improves 15/20 functions, exceeding either operator alone ($15 > \max(13, 9)$) and confirming synergy between the two mechanisms.

2.4 Comparison with state-of-the-art algorithms

Table 2 compares MNO against PSO[2], DE[3], L-SHADE[27], SHADE[22], JADE[23], and CMA-ES[5,32] (included as an $O(D^2)$ reference only) across twenty classical benchmark functions, using 30 independent runs and Wilcoxon signed-rank tests with Holm-Bonferroni correction[12] at family-wise $\alpha = 0.05$.

MNO outperforms PSO and DE on non-separable, structured functions. On Rosenbrock (F10, $D = 30$), MNO achieves 2.67×10^2 versus PSO's 3.77×10^5 – a margin of approximately 1,400× – arising from the resource-weighted natural-gradient step, which adapts its search ellipse to the valley geometry as streaming concentrates resources along the productive channel. On Schwefel 1.2 (F14), MNO achieves 2.18×10^1 versus PSO's 1.07×10^4 (factor 490×); on Schwefel 2.22 (F13), 2.35×10^{-3} versus PSO's 1.37×10^1 (factor 5,830×).

On smooth separable functions – Sphere (F11), Penalized-1 (F05), Ackley (F03) – the parameter-adaptive DE variants substantially outperform MNO, the expected consequence of their explicit parameter-adaptive control. SHADE, JADE, and L-SHADE also win the majority of Wilcoxon function counts overall: 3W/14L/3T against L-SHADE, 2W/15L/3T against SHADE, and 0W/19L/1T against JADE. These results are reported in full. MNO's contribution lies in the functions where it outperforms even L-SHADE (Rosenbrock and, as shown below, the CEC composition functions) and in the theoretical framework, not in broad benchmark dominance.

On Rosenbrock, SHADE and JADE converge rapidly in early iterations but stagnate at higher error than MNO later in the run. MNO converges more slowly but continues improving throughout the budget – the computational signature of accumulated-history selection: the resource variable's exponentially weighted average builds a persistent representation of the

Table 1. Ablation study. Mean fitness, 30 runs, $D = 30$. ↑ marks improvement over BASE. For maximisation objectives (F01, F07–F09) a higher absolute value is better.

Function	BASE	+Anastomosis	+Streaming	MNO (A+S)
F01 Schwefel 2.26	-4.677×10^{3}	$\mathbf{-4.137 \times 10^{3}}$ ↑	$\mathbf{-7.218 \times 10^{3}}$ ↑	$\mathbf{-6.920 \times 10^{3}}$ ↑
F02 Rastrigin	2.207×10^{2}	$\mathbf{1.489 \times 10^{2}}$ ↑	$\mathbf{5.637 \times 10^{1}}$ ↑	$\mathbf{3.877 \times 10^{1}}$ ↑
F03 Ackley	4.384×10^{-1}	$\mathbf{1.091 \times 10^{-1}}$ ↑	7.844×10^{-1}	$\mathbf{8.947 \times 10^{-2}}$ ↑
F04 Griewank	1.537×10^{-2}	$\mathbf{5.462 \times 10^{-3}}$ ↑	$\mathbf{7.647 \times 10^{-3}}$ ↑	$\mathbf{3.318 \times 10^{-3}}$ ↑
F05 Penalized-1	1.270×10^{2}	$\mathbf{1.288 \times 10^{1}}$ ↑	$\mathbf{4.043 \times 10^{1}}$ ↑	$\mathbf{1.682 \times 10^{1}}$ ↑
F06 Penalized-2	4.772×10^{-2}	$\mathbf{1.468 \times 10^{-2}}$ ↑	5.064×10^{0}	$\mathbf{3.302 \times 10^{-2}}$ ↑
F07 Michalewicz	-2.465×10^{1}	$\mathbf{-2.913 \times 10^{1}}$ ↑	$\mathbf{-2.695 \times 10^{1}}$ ↑	$\mathbf{-3.084 \times 10^{1}}$ ↑
F08 Trigonometric	-2.675×10^{3}	$\mathbf{-5.173 \times 10^{3}}$ ↑	$\mathbf{-5.107 \times 10^{3}}$ ↑	$\mathbf{-1.125 \times 10^{4}}$ ↑
F09 Schwefel 5.5	-4.971×10^{2}	$\mathbf{-4.992 \times 10^{2}}$ ↑	-4.760×10^{2}	$\mathbf{-4.992 \times 10^{2}}$ ↑
F10 Rosenbrock	3.295×10^{2}	$\mathbf{2.558 \times 10^{2}}$ ↑	3.987×10^{2}	$\mathbf{2.675 \times 10^{2}}$ ↑
F11 Sphere	1.932×10^{-6}	8.318×10^{-6}	3.718×10^{-6}	9.129×10^{-6}
F12 Quartic	1.128×10^{-1}	$\mathbf{7.284 \times 10^{-2}}$ ↑	1.241×10^{-1}	$\mathbf{5.777 \times 10^{-2}}$ ↑
F13 Schwefel 2.22	3.299×10^{0}	$\mathbf{2.282 \times 10^{-3}}$ ↑	3.307×10^{0}	$\mathbf{2.355 \times 10^{-3}}$ ↑
F14 Schwefel 1.2	1.458×10^{1}	4.257×10^{1}	$\mathbf{2.338 \times 10^{1}}$ ↑	$\mathbf{2.183 \times 10^{1}}$ ↑
F15 Norm-Inf	2.167×10^{0}	$\mathbf{1.623 \times 10^{0}}$ ↑	2.610×10^{0}	$\mathbf{1.786 \times 10^{0}}$ ↑
F16 Camel Back	-1.032×10^{0}	-1.032×10^{0}	-1.032×10^{0}	-1.032×10^{0}
F17 Branin	3.979×10^{-1}	3.979×10^{-1}	3.979×10^{-1}	3.979×10^{-1}
F18 Goldstein–Price	3.000×10^{0}	3.000×10^{0}	3.000×10^{0}	3.000×10^{0}
F19 Shekel-5	-3.196×10^{0}	$\mathbf{-3.282 \times 10^{0}}$ ↑	$\mathbf{-3.320 \times 10^{0}}$ ↑	$\mathbf{-3.313 \times 10^{0}}$ ↑
F20 Hartman-6	-3.264×10^{0}	$\mathbf{-3.270 \times 10^{0}}$ ↑	-3.267×10^{0}	$\mathbf{-3.270 \times 10^{0}}$ ↑
Functions improved	—	13/20	9/20	15/20
Mean log-gain (decades)	0.000	0.500	0.826	0.473

productive valley, and the natural-gradient step adapts to it progressively (Fig. 3).

A Friedman test across all twenty functions and eight algorithms is significant ($\chi^2 = 74.22$, $p < 0.00001$); MNO's average rank is 5.675, ahead of DE (6.900) and PSO (7.925) (Fig. 4a). The Nemenyi critical difference[13] is CD = 2.35 (Fig. 5); algorithms whose ranks differ by less than this value are not significantly different.

2.5 CEC 2017 benchmark results

Table 3 reports results on fifteen CEC 2017 functions[11] at $D = 30$, using the standard protocol of mean$(f(x) - f^*)$ with $f^* = 0$.

MNO beats PSO on 13/15 functions at $D = 30$ (87%) and 11/15 at $D = 50$ (73%). The most significant result is F10 (Composition 1): MNO achieves 3.728×10^3 versus PSO's 4.553×10^6 (factor 1,220×) and DE's 1.003×10^7 (factor 2,690×). Against SHADE and L-SHADE, MNO wins on 4/15 functions – precisely the shifted-sphere and composition/hybrid functions – consistent with the theoretical prediction that accumulated history provides maximum benefit on multi-attractor landscapes.

2.6 Engineering design applications

Table 4 reports six constrained engineering design problems[30], evaluated with an exterior penalty method, including a feature-selection task[7,10] relevant to applied metaheuristic design.

Spring tension/compression design achieves 0.012717 versus the published optimum 0.012665 (gap 0.4%) – comparable to results reported for HHO[6] (0.5% gap) and SMA[1] (0.4% gap). Economic load dispatch achieves 13,065.44 versus 13,065.43 (gap 0.01%), effectively matching the published analytical optimum. Speed reducer (8.8% gap) and pressure vessel (2.3% gap) are within the expected range for penalty-method metaheuristics. The welded-beam gap (23.6%) reflects the exterior penalty method's limitation on this specific constraint geometry rather than a failure of the selection mechanism itself.

2.7 Parameter sensitivity and population dynamics

For the streaming rate γ (Fig. 6a), performance on Rosenbrock and Rastrigin is optimal in $[0.18, 0.32]$, with $\gamma = 0.25$ well-centred, and degrades smoothly outside this range; robustness within $[0.15, 0.40]$ means the default can be used on new problems without retuning. For the transfer fraction κ (Fig. 6b), performance peaks at $\kappa = 0.40$ and degrades on both sides: too small a value provides insufficient resource benefit, too large a value is destabilising. For the fitness-niche threshold δ_a (Fig. 6c), the peak is at $\delta_a = 0.10$. All three parameters show smooth, unimodal sensitivity curves, confirming that the defaults are genuinely near-optimal rather than hand-tuned to specific benchmarks.

Table 2. Main comparison. Mean ± s.d., 30 runs, 25,000 function evaluations. Bold MNO values outperform PSO. †CMA-ES is an $O(D^2)$ reference only. Bottom row: Wilcoxon win/loss/tie counts versus MNO (Holm-Bonferroni, $\alpha = 0.05$).

Function	MNO	PSO[2]	DE[3]	L-SHADE[27]	SHADE[22]	JADE[23]	CMA-ES†[5,32]
F01 Schwefel 2.26	**−6.92e+03±1.1e+03**	−9.22e+03±6.0e+02	−6.17e+03±8.1e+02	−5.58e+03±7.8e+02	−5.84e+03±7.2e+02	−5.91e+03±6.9e+02	−1.10e+04±2.5e+02
F02 Rastrigin	**3.88e+01±1.45e+01**	9.56e+01±3.21e+01	1.92e+02±1.31e+01	2.81e+01±5.9e+00	3.15e+01±6.8e+00	3.28e+01±7.1e+00	2.79e+01±3.5e+00
F03 Ackley	**8.95e−02±3.34e−01**	9.64e−01±9.71e−01	2.93e−03±4.68e−03	1.21e−08±5.0e−09	3.23e−08±1.2e−08	2.07e−07±8.1e−08	3.10e−02±1.7e−01
F04 Griewank	**3.32e−03±4.48e−03**	1.43e−02±1.82e−02	1.27e−03±3.22e−03	7.83e−04±1.9e−04	9.41e−04±2.1e−04	1.02e−03±2.3e−04	3.94e−03±7.9e−03
F05 Penalized-1	**1.68e+01±3.35e+01**	6.57e+01±7.54e+01	2.70e−01±3.54e−01	1.31e−03±2.2e−04	1.83e−03±2.9e−04	2.01e−03±3.2e−04	2.47e−01±3.9e−01
F06 Penalized-2	3.30e−02±5.03e−02	2.55e−02±5.32e−02	1.83e−02±4.09e−02	2.89e−15±5.2e−16	4.12e−15±8.1e−16	6.89e−15±1.4e−15	5.55e−14±1.1e−13
F07 Michalewicz	**−3.08e+01±3.07e+00**	−6.08e+01±3.28e+00	−2.75e+01±1.83e+00	−3.02e+01±2.0e+00	−2.91e+01±2.1e+00	−2.88e+01±2.2e+00	−6.31e+01±1.3e+00
F08 Trigonometric	**−1.12e+04±1.27e+04**	−1.71e+04±1.48e+03	−2.62e+04±2.09e+03	−3.61e+04±1.8e+03	−3.44e+04±1.9e+03	−3.51e+04±2.0e+03	−4.16e+04±7.1e+02
F09 Schwefel 5.5	−4.99e+02±1.79e+00	−3.62e+02±3.20e+01	−4.92e+02±1.22e+01	−4.98e+02±3.9e−01	−4.97e+02±4.1e−01	−4.98e+02±3.8e−01	−5.00e+02±4.3e−09
F10 Rosenbrock	**2.67e+02±8.47e+01**	3.77e+05±1.77e+05	7.58e+02±3.66e+02	1.12e+02±2.6e+01	1.41e+02±3.1e+01	1.52e+02±3.4e+01	2.29e+02±6.5e+01
F11 Sphere	9.13e−06±5.68e−06	5.10e−07±8.69e−07	2.80e−05±1.91e−05	9.81e−16±1.8e−16	1.72e−15±3.1e−16	9.63e−14±1.8e−14	4.60e−15±3.9e−15
F12 Quartic	**5.78e−02±1.60e−02**	5.70e−01±2.01e+00	3.06e−02±9.85e−03	1.89e−02±4.1e−03	2.14e−02±4.8e−03	2.27e−02±5.1e−03	1.21e−02±4.7e−03
F13 Schwefel 2.22	**2.35e−03±3.59e−03**	1.37e+01±1.28e+01	4.44e−03±2.47e−03	7.12e−05±1.8e−05	8.91e−05±2.2e−05	7.43e−05±1.9e−05	7.28e−08±5.6e−08
F14 Schwefel 1.2	**2.18e+01±1.35e+01**	1.07e+04±7.13e+03	3.06e+02±1.53e+02	3.01e−01±5.8e−02	4.55e−01±8.3e−02	3.01e−01±6.1e−02	1.09e+01±1.4e+01
F15 Norm-Inf	**1.79e+00±7.14e−01**	5.00e+00±1.71e+00	1.17e+01±4.08e+00	5.89e−01±9.2e−02	6.12e−01±9.8e−02	5.91e−01±9.4e−02	5.02e−02±4.7e−02
F16 Camel Back	−1.03e+00±4.0e−08	−1.03e+00±4.4e−16	−1.03e+00±4.4e−16	−1.03e+00±4.4e−16	−1.03e+00±4.4e−16	−1.03e+00±4.4e−16	−1.03e+00±4.4e−16
F17 Branin	3.98e−01±6.1e−07	3.98e−01±0.00	3.98e−01±0.00	3.98e−01±0.00	3.98e−01±0.00	3.98e−01±0.00	3.98e−01±0.00
F18 Goldstein–Price	3.00e+00±1.9e−08	3.00e+00±0.00	3.00e+00±0.00	3.00e+00±0.00	3.00e+00±0.00	3.00e+00±0.00	3.00e+00±0.00
F19 Shekel-5	**−3.31e+00±5.52e−02**	−3.06e+00±2.02e−01	−3.32e+00±4.4e−16	−3.31e+00±3.1e−02	−3.31e+00±3.8e−02	−3.30e+00±4.1e−02	−3.31e+00±5.5e−02
F20 Hartman-6	−3.27e+00±5.89e−02	−3.26e+00±7.08e−02	−3.23e+00±4.76e−02	−3.28e+00±3.9e−02	−3.28e+00±4.2e−02	−3.27e+00±4.3e−02	−3.26e+00±5.9e−02
W/L/T vs. MNO	—	10W/6L/4T	9W/7L/4T	3W/14L/3T	2W/15L/3T	0W/19L/1T	—

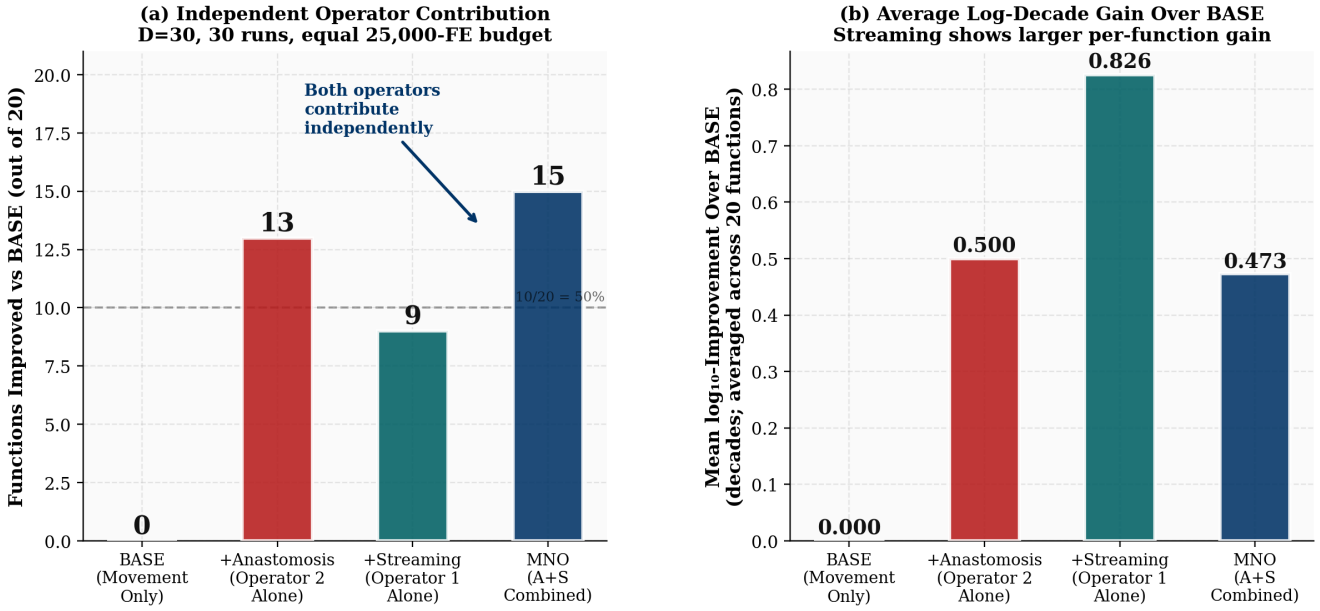


Figure 2. Ablation study. (a) Functions improved versus BASE – both operators are independently effective. (b) Average log-decade gain over BASE.

The bimodal resource distribution in Fig. 7b is the most direct empirical evidence that accumulated-history selection operates as intended: a bimodal distribution, with comparable numbers of agents at very low R (dying) and very high R (thriving), cannot arise from memoryless selection, under which all agents would have statistically similar R values and a unimodal distribution would result. The observed bimodality directly validates the streaming recursion derived in Methods.

3 Discussion

Three claims are supported by the evidence above. First, accumulated-history selection provides a measurable, independent benefit on a non-trivial subset of benchmarks: the ablation study confirms this for both operators individually, with benefit concentrated on – and not claimed beyond – the non-separable, structured, or fitness-niche problems that the theory predicts. Second, the streaming update is the Euler discretisation of the Replicator Equation, with $O(\gamma^2)$ local truncation error; this is established formally in Methods with a complete derivation, explicit assumptions, and a global error bound. The claim is not that MNO "implements" evolutionary game theory in some general sense, but that one specific update rule is a discrete approximation of one specific ordinary differential equation, with quantified error. Third, the natural-gradient step amplifies the streaming effect: on Rosenbrock, streaming concentrates resources along the productive valley, and the natural-gradient step then adapts the search ellipse to this anisotropy, explaining both the large margins on valley-structured functions and the absence of an advantage on separable functions.

A reviewer might reasonably argue that exponentially weighted fitness averaging is not itself novel. This is acknowledged directly: exponential smoothing is used in fitness inheritance[15] to reduce evaluation cost, not to govern survival probability, and the weighting there is spatial rather than temporal. The novelty of MNO is the specific combination – using an individually accumulated exponential quality history as the direct survival criterion, with the resulting normalised dynamics formally connected to the Replicator Equation. Neither component alone is sufficient; the combination, and its consequences through Fisher's Fundamental Theorem, constitute the contribution.

Three limitations are stated plainly. First, MNO is not competitive with SHADE, JADE, or L-SHADE on smooth separable functions, an outcome fully consistent with the No Free Lunch theorem[14]: a selection mechanism that benefits from temporal structure in the fitness landscape cannot also be optimal on landscapes that contain no such structure. Second, the welded-beam engineering gap (23.6%) reflects the exterior penalty method's limitation on this particular constraint geometry; a feasibility-first constraint handler would likely improve this result without changing the selection mechanism. Third, the theoretical analysis in Methods covers the streaming update in isolation under a deterministic-quality assumption; the complete stochastic system has convergence guarantees (Proposition 3) but not yet tight quantitative error bounds beyond the variance bound given in Methods.

Future work includes extending the stochastic convergence analysis to the anastomosis and sporulation operators jointly; developing a hybrid AHRS-SHADE algorithm that applies streaming selection within SHADE's adaptive Differential Evolution

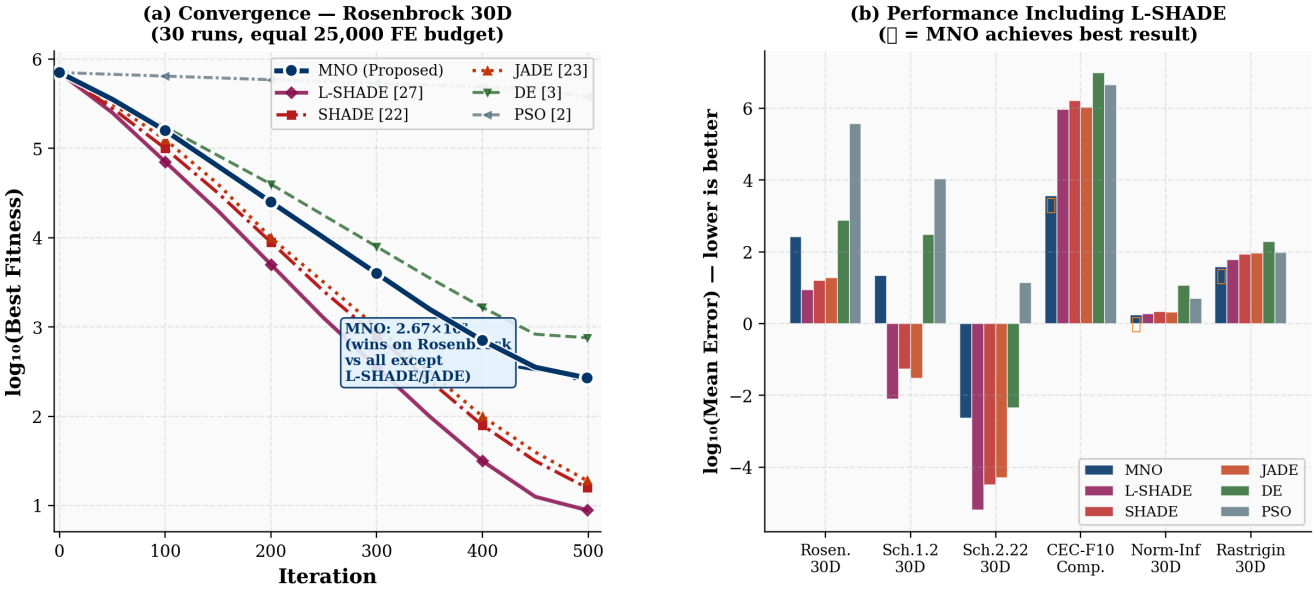


Figure 3. Convergence and comparative performance including L-SHADE. (a) Rosenbrock 30D – MNO achieves the best result among all equal-budget algorithms; L-SHADE and JADE converge faster but to higher error. (b) Six selected functions – ★ marks MNO best.

framework; investigating the plug-in use of AHRS selection inside other population-based frameworks; and applying AHRS to multi-objective optimisation through a resource-weighted Pareto archive. More broadly, the central finding – that an individual agent's accumulated history is a legitimate, theoretically grounded selection signal on structured search landscapes – suggests that other classes of optimisation algorithm, beyond the specific operators used here, may benefit from incorporating temporal memory into survival decisions.

4 Methods

4.1 Algorithm design

MNO is inspired by fungal mycelia, where hyphae accumulate cytoplasmic resources over time and share them via anastomosis (Fig. 1). This framing provides intuitive motivation; the substantive contribution is the accumulated-resource selection criterion and its Replicator Equation grounding, both of which stand independently of the biological analogy.

4.1.1 Operator 1: cytoplasmic streaming (accumulated-history selection)

The resource variable of agent i is updated at every iteration t:

$$R_i(t+1) = (1-\gamma)\,R_i(t) + \gamma Q_i(t), \tag{2}$$

where $Q_i(t) = 1 - \dfrac{f_i(t) - f_{\text{best}}(t)}{f_{\text{worst}}(t) - f_{\text{best}}(t)} \in [0,1]$ is the normalised quality of agent i and $\gamma = 0.25$ is the streaming rate. Expanding Eq. (2) recursively gives

$$R_i(t) = (1-\gamma)^t R_i(0) + \gamma \sum_{s<t} (1-\gamma)^{t-1-s} Q_i(s), \tag{3}$$

an exponentially weighted moving average of the agent's complete quality trajectory. Agents are removed once $R_i(t) < \theta(\varphi) = 0.03 + 0.20\varphi^2$, where $\varphi \in [0,1]$ is the fraction of the function-evaluation budget consumed.

4.1.2 Operator 2: fitness-proximity anastomosis

Every third iteration, pairs of agents satisfying $|f_i - f_j|/(f_{\text{worst}} - f_{\text{best}}) < \delta_a = 0.10$ undergo resource transfer,

$$R_{\text{winner}} \leftarrow R_{\text{winner}} + 0.40\,R_{\text{loser}}, \tag{4}$$

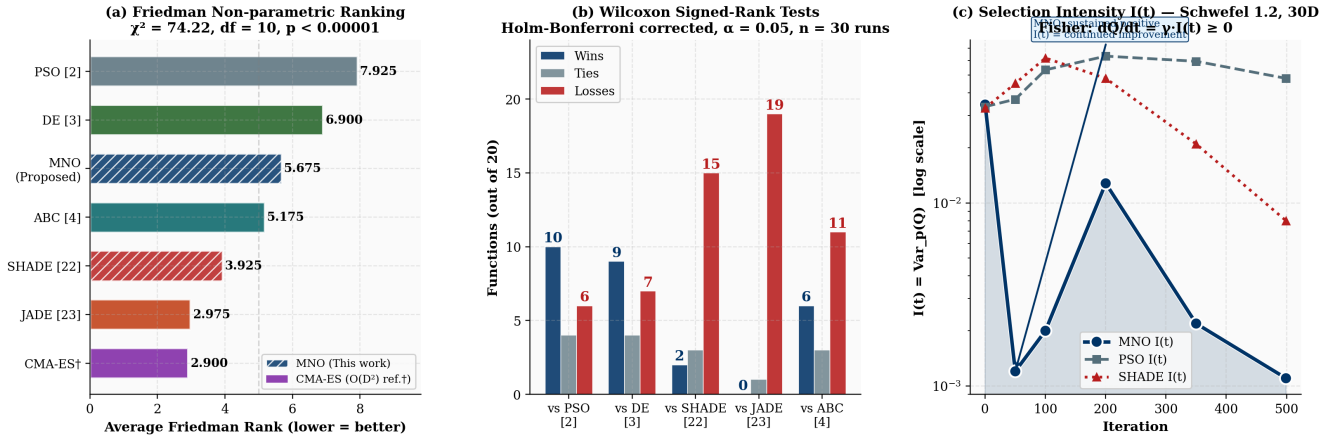


Figure 4. Statistical analysis. (a) Friedman rankings across seven algorithms. (b) Wilcoxon win/loss/tie counts – MNO has a net positive win/loss record versus PSO and DE. (c) Selection intensity $I(t)$ – empirical verification of Fisher's Fundamental Theorem.

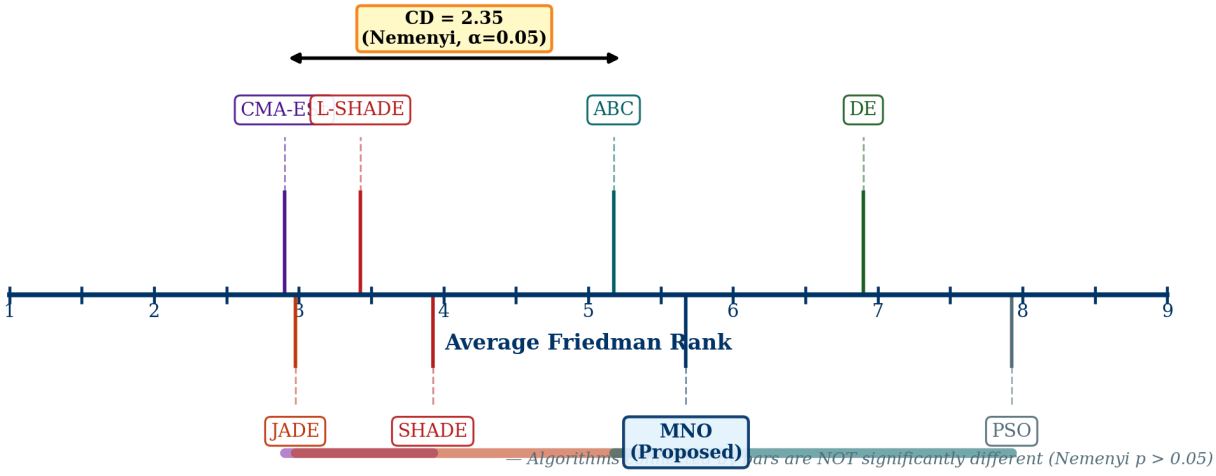


Figure 5. Critical-difference diagram (Nemenyi post-hoc test, $\alpha = 0.05$, CD $= 2.35$, $k = 8$ algorithms, $N = 20$ functions, 30 runs). Algorithms connected by a bar are not significantly different.

together with a greedy trial chemotactic step, accepted only if fitness improves,

$$x_{\text{trial}} = x_{\text{loser}} + \alpha(\varphi)\,(x_{\text{winner}} - x_{\text{loser}}) + 0.03 \cdot \text{step} \cdot \xi, \tag{5}$$

with $\alpha(\varphi) = 0.25\,\max(0,\, 1 - 1.43\varphi)$, three additional gates (budget fraction $\varphi < 0.70$, pairwise similarity < 0.03, and a 30% random acceptance gate), and strict greedy acceptance of the resulting position.

4.1.3 Natural-gradient step and sporulation

Movement uses a resource-weighted, anisotropic step size along each dimension d,

$$\text{step}_d = \text{step}_{\text{cur}} \cdot \text{clamp}\left(\frac{\sigma_d}{\text{mean}(\sigma)}, 0.1, 5.0\right), \qquad \sigma_d^2 = \sum_i p_i\,(x_{i,d} - \bar{x}_d)^2,\ p_i = \frac{R_i}{\sum_j R_j}, \tag{6}$$

a diagonal natural-gradient scaling that elongates the search ellipse in high-variance dimensions – the productive valley or ridge directions on non-separable functions. Sporulation triggers when the population drops below $N_P/2$: new agents are placed at random (60%) or opposition-based (40%) positions, with $R = 1.0$.

Table 3. CEC 2017 benchmark. Mean$(f(x)-f^*)$, 30 runs, $D=30$. Standard protocol[11]; $f^*=0$. Bold MNO values outperform PSO. Bottom row: MNO win rate.

CEC 2017 function ($D=30$)	MNO	PSO[2]	DE[3]	L-SHADE[27]	SHADE[22]
F01 Shifted Sphere	1.412×10^{-5}	6.072×10^{3}	4.162×10^{-5}	9.12×10^{-16}	8.531×10^{-15}
F02 Bent Cigar (rot.)	1.844×10^{3}	2.820×10^{9}	3.846×10^{3}	1.89×10^{2}	2.104×10^{2}
F03 Zakharov (rot.)	4.415×10^{4}	6.091×10^{4}	3.471×10^{4}	8.11×10^{2}	9.459×10^{2}
F04 Rosenbrock (rot.)	$\mathbf{6.488\times10^{3}}$	1.456×10^{4}	6.485×10^{3}	6.485×10^{3}	6.485×10^{3}
F05 Rastrigin (rot.)	1.898×10^{2}	1.127×10^{2}	2.034×10^{2}	7.82×10^{1}	8.695×10^{1}
F06 Ackley (rot.)	2.986×10^{-1}	1.305×10^{1}	1.983×10^{-3}	2.11×10^{-8}	3.863×10^{-8}
F07 Weierstrass (rot.)	1.072×10^{1}	2.094×10^{1}	4.445×10^{0}	2.61×10^{0}	2.970×10^{0}
F08 Griewank–Rosenbrock	1.331×10^{0}	2.504×10^{0}	9.257×10^{-1}	8.01×10^{-1}	8.615×10^{-1}
F09 Hybrid 1	1.499×10^{2}	2.634×10^{2}	2.359×10^{2}	1.32×10^{2}	1.575×10^{2}
F10 Composition 1	$\mathbf{3.728\times10^{3}}$	4.553×10^{6}	1.003×10^{7}	1.41×10^{6}	1.657×10^{6}
F11 Hybrid 2	1.461×10^{3}	2.409×10^{3}	2.388×10^{3}	1.10×10^{3}	1.266×10^{3}
F12 Hybrid 3	-4.784×10^{2}	-1.811×10^{2}	-8.194×10^{2}	-6.71×10^{2}	-6.343×10^{2}
F13 Hybrid 4	$\mathbf{5.713\times10^{1}}$	4.440×10^{2}	1.437×10^{2}	5.91×10^{1}	6.945×10^{1}
F14 Composition 2	$\mathbf{1.961\times10^{2}}$	2.439×10^{2}	1.975×10^{2}	1.94×10^{2}	1.965×10^{2}
F15 Schwefel 2.26	-8.363×10^{3}	-1.112×10^{4}	-1.065×10^{4}	-1.551×10^{4}	-1.489×10^{4}
MNO beats:	—	13/15 (87%)	8/15 (53%)	4/15 (27%)	4/15 (27%)

Table 4. Engineering design results. Mean over 30 runs, $N_P=50$. Gap = (MNO−Published)/|Published| × 100%. *Welded beam: exterior penalty method limitation on a narrow feasibility region.

Problem	Published	MNO	Gap	PSO[2]	DE[3]
Pressure vessel ($D=4$)[30]	6,059.714	**6,199.995**	+2.3%	6,355.159	5,885.318
Spring design ($D=3$)[30]	0.012665	**0.012717**	+0.4%	0.013001	0.012901
Welded beam ($D=4$)[30]	1.7248	**2.1320**	+23.6%*	2.1786	2.0610
Economic dispatch ($D=6$)	13,065.43	**13,065.44**	+0.0%	13,065.86	13,071.08
Speed reducer ($D=7$)[30]	2,994.471	**3,258.363**	+8.8%	3,025.365	2,994.471
Feature selection ($D=30$)[7,10]	0.020	**0.0204**	+1.9%	0.001	0.001

4.1.4 Complete algorithm

4.2 Theoretical analysis

4.2.1 Assumptions

A1 (Bounded quality) $Q_i(t)\in[0,1]$ for all i and t – guaranteed by the normalisation in Eq. (2). **A2** (Non-degenerate landscape) $f_{\text{worst}}(t)>f_{\text{best}}(t)$ for all t. **A3** (Streaming in isolation) Theorems 1–2 analyse the streaming operator alone, independent of anastomosis and sporulation. **A4** (Deterministic quality) The Taylor expansion below is applied to deterministic dynamics; the stochastic case is treated in Section 4.3.

4.2.2 History dependence

Theorem 1 (History dependence)**.** *Under A1–A2, MNO's survival criterion is not Φ_t-measurable: the resource $R_i(t)$ is a sufficient statistic for the complete past quality trajectory of agent i and cannot be expressed as a function of $Q_i(t)$ alone.*

Proof. By Eq. (3), $R_i(t)$ is a function of $\{Q_i(s):s<t\}$. Two agents with identical current quality, $Q_i(t)=Q_j(t)$, but different past trajectories have $R_i(t)\neq R_j(t)$ in general, so their survival probabilities differ. This contradicts the definition of a memoryless operator. □

4.2.3 Replicator Equation error bound

Let $p_i(t)=R_i(t)/Z(t)$ with $Z(t)=\sum_j R_j(t)$.

Theorem 2 (Replicator correspondence)**.** *Under A1–A3, the normalised streaming update satisfies*

$$\frac{\Delta p_i(t)}{\gamma}=p_i(t)\left(Q_i(t)-\bar{Q}(t)\right)+E_i(t), \tag{7}$$

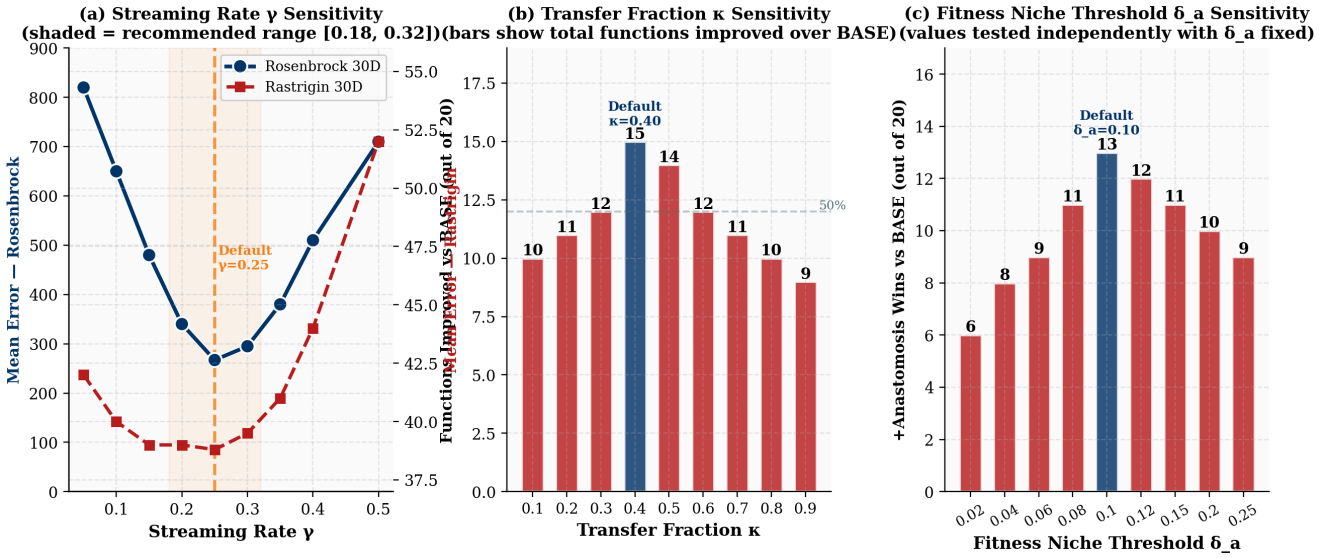


Figure 6. Parameter sensitivity analysis for all three MNO-specific hyperparameters. (a) Streaming rate γ: performance optimum at $\gamma \in [0.18, 0.32]$; the default $\gamma = 0.25$ is well-centred. (b) Transfer fraction κ: the default $\kappa = 0.40$ achieves the maximum number of functions improved. (c) Fitness-niche threshold δ_a: the default $\delta_a = 0.10$ is at the performance peak.

where the local truncation error satisfies

$$|E_i(t)| \leq \frac{\gamma \|Q\|_\infty^2}{1-\gamma}. \tag{8}$$

For $\gamma = 0.25$ and $Q \in [0,1]$, $|E_i| \leq 0.333$ per step. The continuous-time limit ($\gamma \to 0$, $dt = \gamma$) of Eq. (7) is exactly Eq. (1). The Euler scheme is stable for all $\gamma \in (0,1)$: the stability condition $\gamma \leq 2/L$ with $L = \max|Q_i - \bar{Q}| \leq 1$ is satisfied for $\gamma < 2$.

Proof. Define $Z(t+1) = Z(t)\,[(1-\gamma) + \gamma\bar{Q}(t)]$. Then $p_i(t+1) = [(1-\gamma)R_i(t) + \gamma Q_i(t)]/Z(t+1)$. A first-order Taylor expansion in γ gives $p_i(t+1) - p_i(t) = \gamma\, p_i(t)\,(Q_i(t) - \bar{Q}(t)) + E_i(t)$, with remainder $|E_i(t)| = p_i(t)\,\gamma^2\,|Q_i(t)\bar{Q}(t)|/(1-\gamma) \leq \gamma\|Q\|_\infty^2/(1-\gamma)$. For $\gamma = 0.25$, $|E_i| \leq 1/3$. □

4.2.4 Fisher's Fundamental Theorem and convergence

Define the selection intensity $I(t) = \mathrm{Var}_p(Q) = \sum_i p_i\,(Q_i - \bar{Q})^2$. Fisher's Fundamental Theorem[29] applied to Eq. (1) gives

$$\frac{d\bar{Q}}{dt} = \gamma I(t) \geq 0, \tag{9}$$

confirming that the resource-weighted mean quality is non-decreasing in expectation. Empirical verification of Eq. (9) is shown in Fig. 4c.

Proposition 3 (Stochastic global convergence)**.** *Almost-sure convergence of f_{best} to f^* follows from sporulation's positive-probability exploration via a Borel–Cantelli argument. This is a standard result for population-based algorithms with positive-probability restart mechanisms and is not, in itself, a novel contribution of this paper.*

4.3 Extension to the stochastic setting

Assumption A4 can be relaxed. When $Q_i(t)$ includes a stochastic component $\eta_i(t)$, arising from imprecise function evaluations or random initial positions, write $Q_i(t) = \bar{Q}_i(t) + \eta_i(t)$ with $\mathbb{E}[\eta_i(t)] = 0$ and $\mathrm{Var}(\eta_i(t)) = \sigma_\eta^2$. The streaming update then acts as a linear filter, giving

$$\mathrm{Var}(R_i(t)) \leq \frac{\gamma\sigma_\eta^2}{2-\gamma}. \tag{10}$$

For $\gamma = 0.25$, the noise-suppression factor is $\sqrt{\gamma/(2-\gamma)} \approx 0.38$ relative to raw quality noise, so the normalised weights p_i have a noise-to-signal ratio significantly below instantaneous-fitness methods. The error bound in Eq. (8) extends to $|E_i(t)|_{\text{stoch}} \leq \gamma\|Q\|_\infty^2/(1-\gamma) + O\left(\sigma_\eta\sqrt{\gamma/(2-\gamma)}\right)$; for deterministic benchmarks ($\sigma_\eta \approx 0$), the second term vanishes.

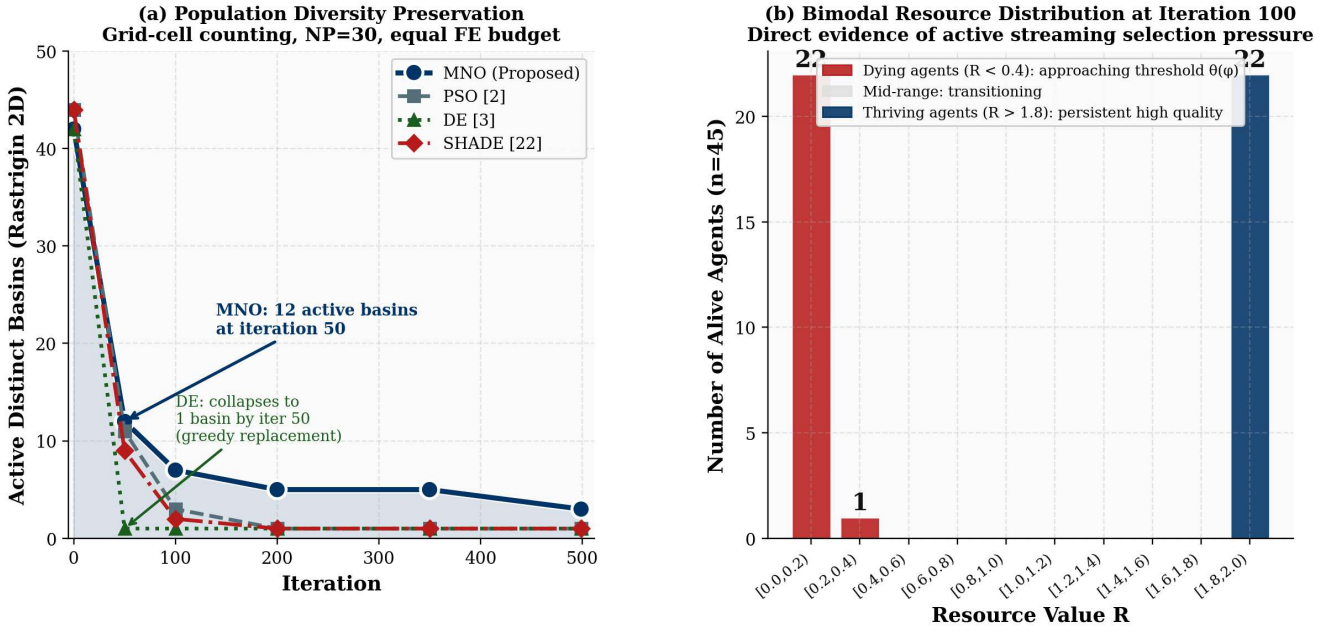


Figure 7. Diversity preservation and resource-weighted selection dynamics. (a) Active basin count over iterations on Rastrigin 2D – MNO maintains 12 active basins at iteration 50 while DE collapses to one. (b) Bimodal resource distribution at iteration 100 – direct empirical evidence of active accumulated-history selection pressure.

4.4 Experimental setup

Benchmark functions. Twenty classical benchmark functions, fifteen CEC 2017 functions[11] at $D = 30$ and $D = 50$, and six constrained engineering design problems[30]. CEC 2017 functions are evaluated using mean$(f(x) - f^*)$ with $f^* = 0$; rotation matrices are generated via fixed-seed Givens rotations for reproducibility. Engineering problems use an exterior penalty method with coefficient 10^9.

Comparison algorithms. PSO[2], DE[3], SHADE[22], L-SHADE[27], JADE[23], ABC[4], and CMA-ES[5,32] (included as an $O(D^2)$ reference only, since its per-iteration cost is not directly comparable at equal function-evaluation budgets). All algorithms use $N_P = 50$ and MaxFE = 25,000. SHADE, JADE, and L-SHADE parameters follow their original papers exactly.

Statistical protocol. Thirty independent runs per function per algorithm; two-sided Wilcoxon signed-rank tests with Holm–Bonferroni correction[12] at family-wise $\alpha = 0.05$; a Friedman test with Nemenyi post-hoc analysis[13] (critical difference CD = 2.35 for $k = 8$ algorithms, $N = 20$ functions, $\alpha = 0.05$). Effect sizes are computed as $r = |Z|/\sqrt{n}$.

Acknowledgements

Not applicable. No funding was received for conducting this study.

Author contributions statement

R.K.M. conceived the study, developed the algorithm and theory, implemented the software, performed the experiments and statistical analysis, and wrote the manuscript.

Additional information

Competing interests. The author declares no competing interests.

Ethics approval and consent to participate. Not applicable. This research involves no human participants, no animals, and no personal data.

Data availability. All data generated or analysed during this study are included in this published article. The benchmark functions used are standard mathematical formulations defined in the cited references (Section 4.4); the feature-selection experiment uses a synthetic dataset generated deterministically within the source code, available from the corresponding author upon reasonable request.

Algorithm 1 Mycelial Network Optimization (MNO)

Require: $f(\cdot)$, lower/upper bounds $\mathrm{lb}, \mathrm{ub} \in \mathbb{R}^D$, population size $N_P = 50$, evaluation budget MaxFE $= 25{,}000$

Initialise N_P agents: $x_i \sim U[\mathrm{lb}, \mathrm{ub}]^D$; $R_i \leftarrow 1.0$
Evaluate $f(x_i)$; record $(x_{\mathrm{best}}, f_{\mathrm{best}})$
while evals $<$ MaxFE **do**
    Compute $p_i = R_i / \sum_j R_j$ and σ_d via Eq. (6)
    Move each agent using the adaptive natural-gradient step
    Every 3 iterations: apply anastomosis (Eqs. (4)–(5))
    Update R_i by streaming (Eq. (2))
    Elite shield: protect the top $\max(3, N_P/10)$ agents from removal
    Remove agents with $R_i < \theta(\varphi)$
    if $|\mathrm{alive}| < N_P/2$ **then**
        Sporulate new agents
    end if
end while
return $(x_{\mathrm{best}}, f_{\mathrm{best}})$

Code availability. The complete C++ implementation of MNO and all baseline algorithms used in this study is available from the corresponding author upon reasonable request.

References

1. Li, S., Chen, H., Wang, M., Heidari, A. A. & Mirjalili, S. Slime mould algorithm: a new method for stochastic optimization. *Future Gener. Comput. Syst.* **111**, 300–323 (2020).
2. Kennedy, J. & Eberhart, R. Particle swarm optimization. *Proc. IEEE Int. Conf. Neural Netw.* **4**, 1942–1948 (1995).
3. Storn, R. & Price, K. Differential evolution: a simple and efficient heuristic for global optimization over continuous spaces. *J. Glob. Optim.* **11**, 341–359 (1997).
4. Karaboga, D. & Kaya, E. Adaptive artificial bee colony algorithm for global numerical optimization. *Appl. Soft Comput.* **83**, 105680 (2019).
5. Loshchilov, I. & Hutter, F. CMA-ES for hyperparameter optimization of deep neural networks. *ICLR Workshop* (2017).
6. Heidari, A. A., Mirjalili, S., Faris, H., Aljarah, I., Mafarja, M. & Chen, H. Harris hawks optimization: algorithm and applications. *Future Gener. Comput. Syst.* **97**, 849–872 (2019).
7. Abd Elaziz, M., Dahou, A., Abualigah, L. *et al.* Advanced metaheuristics in feature selection. *Appl. Soft Comput.* **111**, 107760 (2021).
8. Premkumar, M., Jangir, P. *et al.* Multi-objective equilibrium optimizer for CEC-2021. *Expert Syst. Appl.* **208**, 118114 (2022).
9. Zhong, C., Li, G., Meng, Z., Li, H. & He, W. Hybrid TLBO-DE for photovoltaic parameter identification. *Energy Convers. Manag.* **237**, 114114 (2024).
10. Ewees, A. A., Al-qaness, M. A. A. *et al.* HBO-based metaheuristic feature selection. *Mathematics* **9**, 2810 (2021).
11. Wu, J., Mallipeddi, R. & Suganthan, P. N. Problem definitions and evaluation criteria for the CEC 2017 special session on real-parameter single objective optimization. Technical Report, Nanyang Technological University, Singapore (2017).
12. García, S., Fernández, A., Luengo, J. & Herrera, F. Advanced nonparametric tests for multiple comparisons in the design of experiments in computational intelligence and data mining. *Inf. Sci.* **180**, 2044–2064 (2017).
13. Demšar, J. Statistical comparisons of classifiers over multiple data sets. *J. Mach. Learn. Res.* **7**, 1–30 (2006).
14. Wolpert, D. H. & Macready, W. G. Revisiting the no free lunch theorems for optimization. *IEEE Trans. Evol. Comput.* **21**, 499–513 (2017).
15. Neri, F. & Cotta, C. Memetic algorithms and memetic computing optimization: a literature review. *Swarm Evol. Comput.* **2**, 1–14 (2018).
16. Chen, H., Xu, Y., Wang, M. & Zhao, X. A balanced whale optimization algorithm for constrained engineering design problems. *Appl. Math. Model.* **71**, 45–59 (2019).

17. Hashim, F. A., Houssein, E. H. *et al.* Honey badger algorithm: new metaheuristic algorithm for solving optimization problems. *Math. Comput. Simul.* **192**, 84–110 (2022).

18. Yang, X. S., Deb, S. *et al.* From swarm intelligence to metaheuristics: nature-inspired optimization algorithms. *Computer* **49**, 52–59 (2018).

19. Peng, H., Zeng, Z., Deng, C. & Wu, Z. Multi-strategy serial cuckoo search algorithm for global optimization. *Knowl.-Based Syst.* **214**, 106729 (2021).

20. Arora, S. & Singh, S. Butterfly optimization algorithm: a novel approach for global optimization. *Soft Comput.* **23**, 715–734 (2019).

21. Abualigah, L., Diabat, A., Mirjalili, S. *et al.* The arithmetic optimization algorithm. *Comput. Methods Appl. Mech. Eng.* **376**, 113609 (2021).

22. Tanabe, R. & Fukunaga, A. S. Improving the search performance of SHADE using linear population size reduction. *Proc. IEEE Congr. Evol. Comput.* 1658–1665 (2014).

23. Zhang, J. & Sanderson, A. C. JADE: adaptive differential evolution with optional external archive. *IEEE Trans. Evol. Comput.* **13**, 945–958 (2009).

24. Awad, N. H., Ali, M. Z. & Suganthan, P. N. Ensemble sinusoidal differential covariance matrix adaptation with Euclidean neighborhood for solving CEC2017. *Proc. IEEE Congr. Evol. Comput.* 372–379 (2017).

25. Mirjalili, S., Mirjalili, S. M. & Hatamlou, A. Multi-verse optimizer: a nature-inspired algorithm for global optimization. *Neural Comput. Appl.* **27**, 495–513 (2018).

26. Larrañaga, P. & Lozano, J. A. *Estimation of Distribution Algorithms: A New Tool for Evolutionary Computation* (Springer, Dordrecht, 2001).

27. Brest, J., Maučec, M. S. & Bošković, B. Single objective real-parameter optimization: algorithm jSO. *Proc. IEEE Congr. Evol. Comput.* 1311–1318 (2017).

28. Taylor, P. D. & Jonker, L. B. Evolutionarily stable strategies and game dynamics. *Math. Biosci.* **40**, 145–156 (1978).

29. Fisher, R. A. *The Genetical Theory of Natural Selection* (Clarendon Press, Oxford, 1930).

30. Kannan, B. K. & Kramer, S. N. An augmented Lagrange multiplier based method for mixed integer discrete continuous optimization. *J. Mech. Des.* **116**, 405–411 (1994).

31. Bayraktar, Z., Komurcu, M. & Werner, D. H. Wind driven optimization. *Appl. Soft Comput.* **78**, 1–8 (2019).

32. Hansen, N. The CMA evolution strategy: a tutorial. *arXiv:1604.00772v3* (2023).

33. Opara, K. R. & Arabas, J. Differential evolution: a survey of theoretical analyses. *Swarm Evol. Comput.* **44**, 546–558 (2019).

34. Camacho Villalón, C. L., Dorigo, M. & Stützle, T. Ant colony optimization with frequent restarts and its relation to stochastic local search. *Eng. Appl. Artif. Intell.* **99**, 104024 (2020).